ARTICLE

Controlled arrangement of [2 x 2] metallo-supramolecular grids formed by 4,6-bis((1*H*-1,2,3-triazol-4-yl)-pyridin-2-yl)-2-phenylpyrimidine ligands: from discrete [2 x 2] grid structures to star-shaped supramolecular polymeric architectures

Received 00th January 20xx,
Accepted 00th January 20xx

DOI: 10.1039/x0xx00000x

Xiaowen Xu,[a] Anne K. Seiffert,[a] Ruben Lenaerts,[a] Kanykei Ryskulova,[a] Kristof Van Hecke,[b] Valentin Victor Jerca,[a] and Richard Hoogenboom*[a]

The self-assembly of bis-tridentate ligands leads to the spontaneous formation of [2x2] grid-like metal complexes. However, the synthesis of such ligands is rather cumbersome. In the work, we demonstrate a straightforward synthesis route to prepare bis-tridentate 4,6-bis((1*H*-1,2,3-triazol-4-yl)-pyridin-2-yl)-2-phenylpyrimidine ligands through double CuAAC click chemistry with 4,6-bis(6-ethynylpyridin-2-yl)-2-phenylpyrimidine as well as their self-assembly into [2x2] grid-like metal complexes. In addition, four macromolecular ligands were synthesized starting from azido-end-functionalized poly(2-ethyl-2-oxazoline) (PEtOx) or poly(ethylene glycol) (PEG). These macromolecular ligands were used in the construction of star-shaped supramolecular polymers through complexation with transition metal ions (e.g., Fe^{2+} or Zn^{2+}). The successful fabrication of complexes and star-shaped polymers was confirmed by UV-vis titration measurements and MALDI-TOF mass spectrometry. However, the chemical structure of the polymer was found to have a strong influence on the [2x2] grid formation, which was successful with the PEG-ligands but not with the PEtOx-ligands, while the molecular weight of the PEG did not interfere with grid formation.

Introduction

The self-assembly of complex, multi-component and highly oriented metallo-supramolecular architectures having a variety of tunable and potentially useful characteristics remains a region of extremely active research in supramolecular and/or coordination chemistry.[1] Both polymeric and discrete metallo-supramolecular structures have been reported to show some promising properties, with reported potential applications such as catalysis, magnetism, electrochemistry, photoactivity, and gas separation and absorption.[2] Of them, metal ions-directed grid-type arrangements composed of both spin centers as well as stacking ligands are one of those paramount structural models.[3] The regular array of a set of metal ions has been considered applicable to information storage device.[4] The well-defined supramolecular architectures can be straightforwardly fabricated by the self-assembly of well-designed organic ligands induced by metal ions, arranged from the [2 x 2] to the even [n x n] level (n = 3, 4…), which exhibited intriguing physicochemical behaviors and aesthetically appealing achitectures.[5, 6]

In the design and synthesis of such systems, a continuing requirement remains for the discovery of a family of novel ligands and binding moieties with the aspect of creating dependable archetypal bases from which to establish classes of smart materials by means of molecular precursors. In this respect, various types of organic ligands such as bis(pyridyl)pyridazine,[7] bis(hydrazone),[8, 9] pyrazolate-bridged binucleating ligand,[10] bis-tridentate (1,2,3-triazol-4-yl)-picolinamide,[11] bis(bipyridine)pyrimidine,[12] etc. have been successfully developed to prepare square [2 x 2] grid-like assemblies, mainly with octahedral coordination geometry, in the presence of transition metal ions and/or lanthanide ions. Compared to other ligands, considerable attention has been given to the 4,6-bis(2,2-bipyridyl-6-yl)-2-phenylpyrimidine ligands due to their fascinating structures, magnetic,[13] optical[14] and remarkable electronic properties[15] upon formation of [2 x 2] grid-like complexes in the presence of specific metal ions. However, the synthesis of functionalized 4,6-bis(2,2-bipyridyl-6-yl)-2-phenylpyrimidine ligands is rather cumbersome and the formation of grid like complexes is exclusively limited to the small molecular scale. Ligands designed by combining functional macromolecules from which to potentially prepare self-assembled star-shaped metallo-supramolecular polymers has not been explored to date, although grid-like metal complexes appear to be ideally suited as self-assembled core structure for the preparation of star-shaped polymers.[9, 16-19]

[a] *Supramolecular Chemistry Group, Centre of Macromolecular Chemistry (CMaC), Department of Organic and Macromolecular Chemistry, Ghent University, Krijgslaan 281-S4, B-9000 Ghent, Belgium.*
Email: richard.hoogenboom@ugent.be.
[b] *XStruct, Department of Chemistry, Ghent University, Krijgslaan 281-S3, B-9000, Ghent, Belgium.*

Electronic Supplementary Information (ESI) available: Full experimental details and ^{1}H and ^{13}C NMR spectra. Details of the X-ray analysis of compound **3** (CCDC: 1945081). For ESI and crystallographic data in CIF or other electronic format see DOI: 10.1039/x0xx00000x

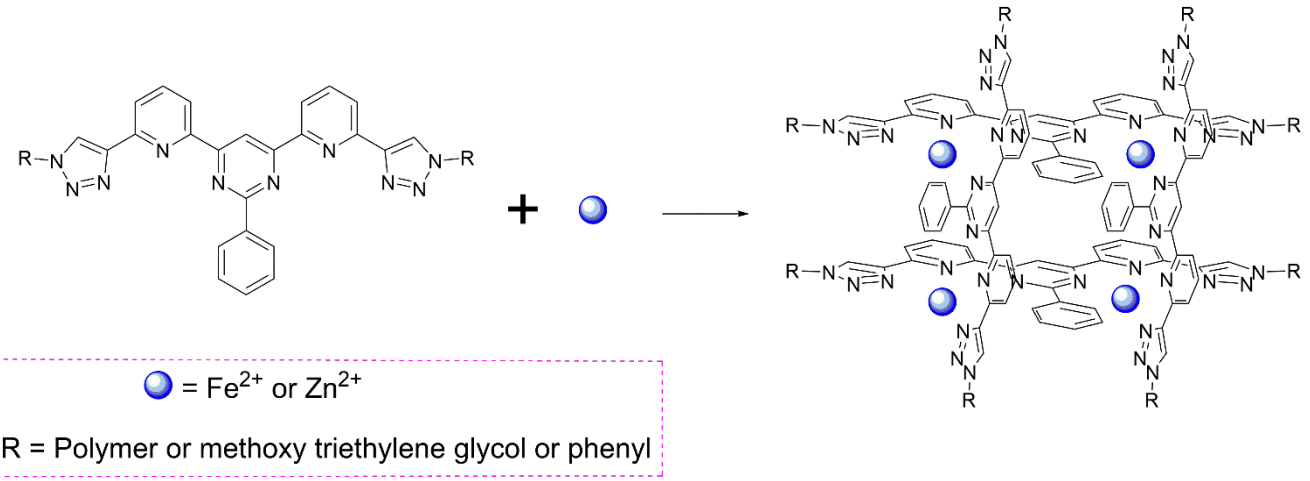

Scheme 1. Structure of the 4,6-bis((1*H*-1,2,3-triazol-4-yl)-pyridin-2-yl)-2-phenylpyrimidine ligands and their complexation into [2x2] grid-like metal complexes with Fe^{2+} or Zn^{2+} salts leading to star-shaped polymers in case of macromolecular ligands.

The recent advances in the copper-catalyzed azide-alkyne cycloaddition (CuAAc) click reaction promoted the use of 1,4-disubstituted-1,2,3-triazoles in coordination chemistry, which has led to the development of 1,2,3-triazole-containing analogues of bipyridine, terpyridine and 3,6-di(2-pyridiyl)-pyridazine metal coordinating ligands.[20-22] The major advantage of replacing one or two pyridine rings with a 1,2,3-triazole ring is the much easier synthesis of functional ligands through CuAAC.

In this work, we hypothesized that the outer pyridine rings of 4,6-bis(2,2-bipyridyl-6-yl)-2-phenylpyrimidine could be replaced by 1,2,3-triazole rings providing a much easier synthetic access to bis-tridentate [2x2] grid-like metal complex forming ligands functionalized with polymer chains as basis for supramolecular star-shaped polymers as shown in Scheme 1. Therefore, the clickable ligand precursor 4,6-bis(6-ethynylpyridin-2-yl)-2-phenylpyrimidine) was first synthesized, followed by CuAAC with two low molar mass azido compounds to demonstrate the synthesis as well as to evaluate whether the novel bis-tridentate 4,6-bis((1*H*-1,2,3-triazol-4-yl)-pyridin-2-yl)-2-phenylpyrimidine ligand can self-assemble into [2x2] grid-like metal complexes in presence of Fe^{2+} or Zn^{2+} metal ions. Next, macromolecular ligands were prepared by CuAAC of 4,6-bis(6-ethynylpyridin-2-yl)-2-phenylpyrimidine) with azido end-functionalized poly(2-ethyl-2-oxazoline) (PEtOx) or poly(ethylene glycol) (PEG). These polymers were chosen due to their water solubility, non-ionic characteristic, and high flexibility of the main chain.[23] Finally, the self-assembly of the macroligands into star-shaped polymer [2x2] grid-like metal complexes in presence of Fe^{2+} or Zn^{2+} metal ions will be discussed (Scheme 1).

Results and discussion

Synthesis and characterization of the 4,6-bis((1*H*-1,2,3-triazol-4-yl)-pyridin-2-yl)-2-phenylpyrimidine ligands

The synthesis procedure for the 4,6-bis((1*H*-1,2,3-triazol-4-yl)-pyridin-2-yl)-2-phenylpyrimidine ligands is outlined in Scheme 2. The ligands were synthesized in four steps from commercially available starting compounds (full details are included in the supporting information). In the first step, compound **1** was obtained by palladium-catalyzed Sonogashira cross-coupling of 2,6-dibromopyridine with triisopropylsilyl (TIPS) acetylene.[24] Next, the product **1** was reacted with *n*-BuLi, and, subsequently, reacted with tributyltin chloride to yield compound **2**.[24] In the third step, a palladium-catalyzed Stille coupling of compound **2** was performed with 4,6-dichloro-2-phenylpyrimidine (fenclorim) to obtain compound **3**, from which a single crystal X-ray structure was obtained (supporting information; Figure S5). The ligands **L1-L6** were prepared in a single final step by *in situ* deprotection of the TIPS-groups of **3** with tetrabutylammonium fluoride (TBAF) and, subsequent, CuAAC click reaction with the azide derivatives. Intermediate purification after the cleavage step was not necessarily due to the high yield of the reaction. The PEtOx-functionalized macroligands **L3-L4** were purified using preparative size exclusion chromatography (Biobeads SX-1), while organic ligands **L1-L2** and PEG-functionalized macroligands **L5-L6**, were purified by silica column chromatography. The removal of copper from the final products was done by dissolving the ligands in dichloromethane and washing with a 5 wt% EDTA aqueous solution. The azido-functionalized PEG and PEtOx were synthesized following previously reported literature procedures

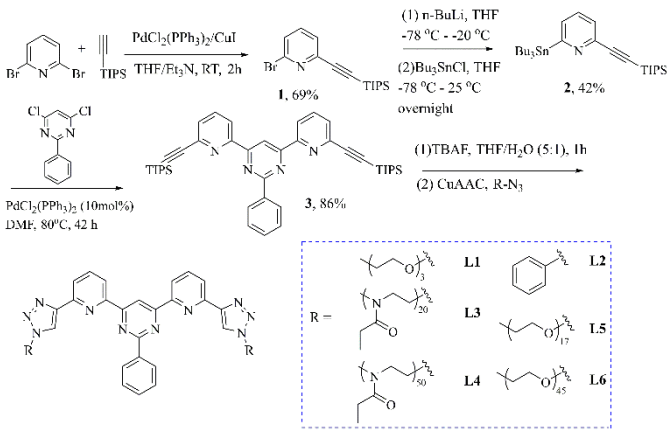

Scheme 2. The synthesis procedure of organic (**L1-L2**), and macromolecular ligands (**L3-L6**) used in this study.

(synthesis details and full characterization are included in the supporting information; molar mass data in Table 1).[25, 26]

Table 1. Number average molecular weight (M_n) and dispersity of the macromolecular ligands and the polymeric precursors. Note that the PEG_{17} derivatives had a too low molar mass to be analysed by SEC.

polymer	$M_{n,\ NMR}$	$M_{n,\ SEC,\ RI}$	$Đ_{SEC,\ RI}$	$M_{n,\ MALDI}$
$PEtOx_{20}$-N_3	2300	3000	1.13	2208
$PEtOx_{50}$-N_3	4900	8800	1.16	4675
PEG_{17}-N_3	/	/	/	805
PEG_{45}-N_3	/	3900	1.05	2039
L3	4300	8800	1.17	4796
L4	9700	17000	1.08	9891
L5	1800	/	/	1622
L6	5000	6500	1.08	4162

The structures of the obtained ligands were confirmed by NMR spectroscopy, and high-resolution mass spectrometry (HRMS) for **L1** and **L2** respectively. The ^{1}H-NMR spectra of **L1** displayed the characteristic signals in the aromatic region (peak a, c, e) corresponding to the protons of the pyrimidine, pyridine rings, and triazole rings, respectively (Figure 1a middle, and Figure S12). Furthermore, the appearance of two triplets (peak f and g) assigned to the methylene groups connected to the triazole ring at 4.71 ppm and 3.96 ppm were observed, respectively. The ^{1}H-NMR spectra of the other ligands showed similar chemical shifts indicating the successful ligand formation through CuAAC (supporting information). Further evidence for the quantitative triazole ring formation was obtained from the FTIR spectroscopy. As shown in Figure S20, the signal corresponding to the azido moieties at 2101 cm^{-1} disappeared after the click reaction.[18, 27, 28] SEC analysis of the purified macromolecular ligands **L3, L4,** and **L6** revealed a monomodal distribution with a narrow dispersity and a distinctive shift in the retention time compared to the corresponding PEtOx-N_3 or PEG-N_3 (Figure S21 and Figure S22). It should be noted that the molecular weight of **L5** and its PEG_{17}-N_3 precursor was too small to be detected by the SEC measurement. Moreover, MALDI-TOF MS also supported the successful preparation of the macroligands **L3-L6**, by a shift of the molar mass distribution to higher, roughly double molar mass (Figure S23). The obtained data from ^{1}H-NMR spectroscopy, SEC, and MALDI-TOF MS for all the macroligands and their precursors is summarized in Table 1. The M_n obtained from ^{1}H-NMR spectroscopy, and MALDI-TOF MS correspond well with the theoretical M_n, while the M_n obtained from SEC deviates due to the use of a relative calibration of the SEC against PMMA standards.

Complexation of ligands L1 and L2 with Fe^{2+} and Zn^{2+} ions

The organic ligand **L1** was selected as a model compound to investigate the complexation behavior with Fe^{2+} and Zn^{2+} ions in CD_3CN by ^{1}H-NMR spectroscopy. Addition of 0.5 equivalents of $Fe(BF_4)_2$ to a solution of **L1** resulted in an instant color change from colorless to red. Further addition of the Fe^{2+} ions up to 1 equivalent of Fe^{2+} led to a second color change from red to blue indicative of the formation of [2x2] grid-like iron(II) complexes.[29] Complexation of **L1** with an equimolar amount of Zn^{2+} in CD_3CN resulted in a yellowish color change. The signals in the ^{1}H-NMR spectrum of Fe^{2+}-**L1** [2x2] complex (Figure 1a, top) are broader and very small due to the paramagnetism of the iron(II) ions, being consistent with the reported literature for related complexes.[18] Nonetheless, a clear chemical shift of the signals corresponding to the ligand can be observed supporting the successful formation of octahedral bis(tridentate) complexes with a grid-like structure. Complexation of **L1** with Zn^{2+} revealed the characteristic upfield shift of the a, n, and o protons and a downfield shift of the b, c, d, and m protons in the ^{1}H-NMR spectrum (Figure 1a, bottom and Figure 1b).[30]

Furthermore, UV-vis titrations were performed to study the complexation of **L1** with Fe^{2+} and Zn^{2+} ions in acetonitrile (Figure 2 and Figure S24). The metal ions were added as metal tetrafluoroborate salts due to their good solubility in acetonitrile. Upon addition of Fe^{2+} ions, the absorption maxima of **L1** shifted from 238 to 266 nm and from 315 to 358 nm, respectively. In addition, the metal ligand charge transfer (MLCT) band appeared at 528 nm (Figure S24). This MLCT absorbance reached a plateau after addition of 1 eq. of Fe^{2+} ions, indicating the expected stoichiometry for a [2x2] grid-like complex. It should be noted that the intensity of the MLCT band is rather weak due to the low concentration of the solution (e.g., $2.3x10^{-5}$ mol/L). Increasing the concentration of **L1** to $3.4x10^{-4}$ mol/L clearly revealed the appearance of the MLCT band at 528 nm (Figure 2a), corresponding to the color change from colorless to red. Further increasing the Fe^{2+} content to 1 eq. led to a shift of

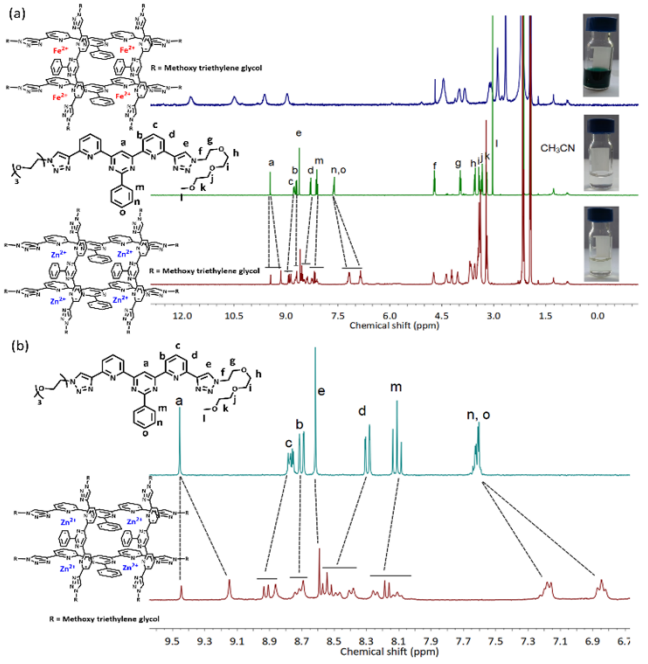

Figure 1. (a) ^{1}H-NMR spectrum of ligand **L1** (middle, CD_3CN), and its corresponding $Fe(BF_4)_2$ complex (top, CD_3CN), as well as $Zn(BF_4)_2^+$ complex (bottom, CD_3CN); (b) the zoom of the aromatic area.

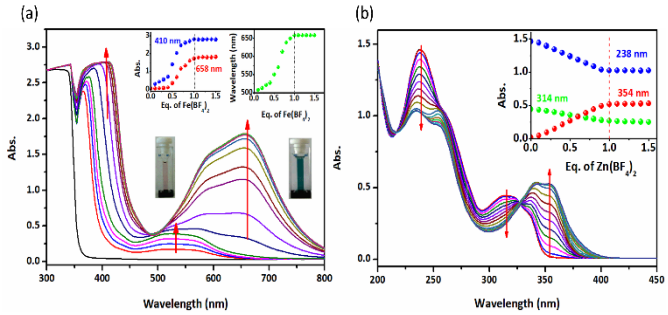

Figure 2. UV-vis spectroscopy titration experiments: (a) stepwise addition of 1 µL of 3.4 x 10^{-2} mol/L of solution of $Fe(BF_4)_2$ to a 3.4 x 10^{-4} mol/L of **L1** in CH_3CN, (b) stepwise addition of 1.9 µL of 1.8 x 10^{-3} mol/L of solution of $Zn(BF_4)_2$ to a 2.3 x 10^{-5} mol/L of **L1** in CH_3CN. The inset graphs show the changes in the absorption with the increase of the amount of transition metal ions.

the MLCT to 658 nm indicating a transition from complexes with two ligands and one Fe^{2+} up to 0.5 equivalents of Fe^{2+} into more stable [2x2] grid-like complexes from 0.5 to 1 equivalent of Fe^{2+} ions, accompanied by a color change from red to blue. Moreover, no significant change of the absorption band was observed after adding more than 1 equivalent of Fe^{2+} ions, suggesting that all of the ligands were fully complexed and that the formed grids are stable (Figure 2a, inset). The observation that the shift in the MLCT band only occurs after addition of 0.5 equivalents of Fe^{2+} indicates that there is no strong cooperativity for the formation of the [2x2] complexes as these are only formed after all ligands have been consumed in complexes with 2 ligands and 1 Fe^{2+} ion.

Upon titration of Zn^{2+} ions to a solution of **L1** in acetonitrile, bathochromic shifts from 238 nm to 260 nm and from 314 nm to 354 nm were observed, respectively. The titration shows a clear isosbestic point indicating that a clean transition from ligands to full [2x2] grid complexes occurs even at low equivalents of Zn^{2+} ions, indicating high cooperativity for the [2x2] grid formation. This higher cooperativity compared to the complexation of **L1** with Fe^{2+} ions may result from the lower stability of the Zn^{2+} complex with one metal ion and two ligands allowing dynamic exchange towards the thermodynamically most stable grid-like structures.[31] The maximum absorption was reached at a 1:1 ratio of Zn^{2+} ions to **L1**, which remained constant upon addition of more Zn^{2+} ions, demonstrating the successful formation of stable [2x2] grid-like complexes (Figure 2b).

Next, MALDI-TOF mass spectroscopy was used to investigate the [2x2] grid-like complex formation. The mass peaks corresponding to $\{[Fe_4\mathbf{L1}_4](BF_4)_n\}^{(8-n)+}$ (n = 4～7) structures were indeed observed in the MALDI-TOF mass spectrum, further confirming the successful formation of the [2x2] grid-like iron complex (Figure 3a). However, MALDI-TOF-MS of the Zn^{2+}-**L1** grid revealed only the molar mass of the complex containing two ligands with one Zn^{2+} ion (i.e., $[Zn\boldsymbol{L1}_2]$), which might be caused by the high laser intensity leading to the fragmentation of the grid (Figure 3b), suggesting that the grid-like complex of **L1** with Fe^{2+} ions is more stable than the grid-like complex of

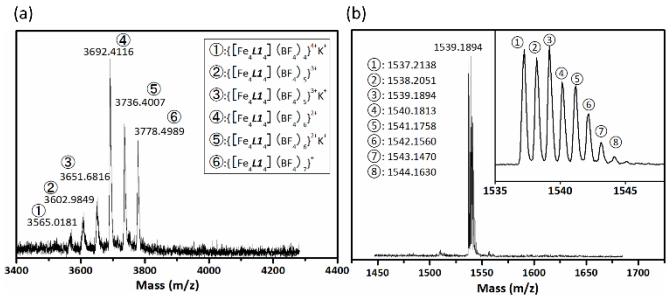

Figure 3. Partial MALDI-TOF mass spectra of the grid-like complexes of **L1** with (a) Fe^{2+}, and (b) Zn^{2+}, respectively.

ligand **L1** with Zn^{2+} ions as both NMR and UV-vis spectroscopy confirmed full complexation of **L1** with Zn^{2+} ions.

Single crystal structures of the Fe^{2+}-**L1** grid-like complexes could unfortunately not be obtained due to the flexible structure of the ligand. Consequently, we synthesized **L2** by replacing the TEG groups with more rigid phenyl rings. However, also with the more rigid ligand **L2** no single crystals could be obtained, because of the precipitation of the complex from CH_3CN. Nevertheless, ^{1}H-NMR spectroscopy revealed the formation of the [2x2] grid-like structure upon addition of 1 equivalent of Fe^{2+} ions or Zn^{2+} ions (Figure S25). The **L2**-M^{2+} complexes showed similar characteristic shifts as previously discussed for the **L1**-M^{2+} complexes (Figure 1).

After establishing the synthesis of the 4,6-bis((1*H*-1,2,3-triazol-4-yl)-pyridin-2-yl)-2-phenylpyrimidine ligands and their successful self-assembly in grid-like metal complexes with Zn^{2+} ions and Fe^{2+} ions, we focused our attention to the self-assembly of the polymeric macroligands **L3-L6** to investigate the formation of supramolecular star-polymers through [2x2] grid-like metal complex formation. The complexation of the PEtOx macroligands **L3** and **L4** was initially studied using UV-vis spectroscopy titrations in CH_3CN. Upon addition of the Fe^{2+} ions the ligand absorption band was red shifted from 300 nm to 348 nm, indicative of metal-ligand complex formation, as previously observed for the complexation of ligand **L1**. However, no distinct MLCT band nor a red or blue coloration of the solution was observed, suggesting that no [2x2] grid-like complexes were formed (Figure S26 a, c). Similar results were found for Zn^{2+} complexes (Figure S26 b, d). It may be speculated that the PEtOx chains provide a too large steric bulk, thereby obstructing the formation of the star-shaped polymeric [2x2] grid-like complexes.

Next, the self-assembly of the PEG macroligands was investigated by UV-vis titration of **L5**, and **L6** with Fe^{2+}, and Zn^{2+} ions as shown in Figure 4. During the titration with Fe^{2+}, the absorption maxima were red shifted as well. Furthermore, the appearance of the characteristic MLCT band of the Fe^{2+} complex with **L5** at 532 nm indicated the formation of polymeric [2 x 2] grids, albeit the MLCT band at 658 nm could not be observed at this lower concentration (Figure 4a), which was also the case for the lower molar mass ligand **L1** (Figure S24). The absorption at 349 nm increased linearly upon addition of Fe^{2+} and the maximum absorption was reached after approximately 1

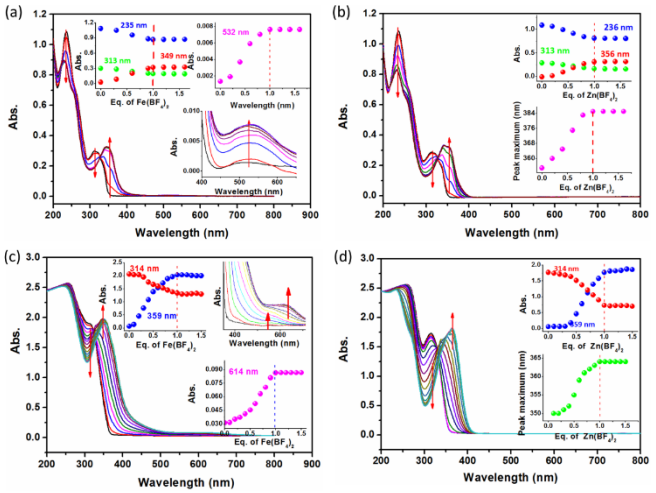

Figure 4. UV-vis spectroscopy titration experiments: (a) stepwise addition of 7.8 µL of 1.43 x 10^{-3} mol/L of solution of $Fe(BF_4)_2$ to a 3.7 x 10^{-5} mol/L of **L5** in CH_3CN, (b) stepwise addition of 6.0 µL of 1.8 x 10^{-3}mol/L of solution of $Zn(BF_4)_2$ to a 3.7 x 10^{-5} mol/L of **L5** in CH_3CN, (c) stepwise addition of 4.8 µL of 1.3 x 10^{-3} mol/L mol/L of solution of $Fe(BF_4)_2$ to a 4.17 x 10^{-5} mol/L of **L6** in CH_3CN, and (d) stepwise addition of 3.4 µL of 1.8 x 10^{-3} mol/L of solution of $Zn(BF_4)_2$ to a 4.17 x 10^{-5} mol/L of **L6** in CH_3CN. The inset graphs show the changes in the absorption with the increase of the amount of transition metal ions.

equivalent of Fe^{2+} corresponding to [2x2] grid formation. One may conclude that the [2x2] grid formation formed by the complexes of **L5** with Fe^{2+} indeed occurs despite of the disappearance of MLCT band at 658 nm due to the low concentration of **L5** solution, which is consistent with the above discussed result of **L1** with Fe^{2+} at low concentration. Increasing the concentration would aid the detection of MLCT band at 658 nm. This assumption was further proved by the successful determination of MLCT band at 658 nm for the complexes of **L6** with Fe^{2+} ions at a high concentration. Regardless of the high molar mass, the absorption maximum of macroligand **L6**, measured at lightly higher concentration than **L5**, shifted from 525 to 658 nm around 0.5 equivalents of Fe^{2+} ions, suggesting a transition from complexes with two ligands and one Fe^{2+} ion into grid-like complexes. Clearly, the chain length of the polymer did not influence the formation of the grids as the maximum of the **L1,** and **L6** also shifted around 0.5 equiv. of Fe^{2+} (Figure S24 and 4c). The titration of the PEG macroligands with Zn^{2+} ions revealed similar absorption band as the lower molar mass [2x2] grid-like complex of **L1** at 356 nm (Figure 4b and 4d). These results clearly indicate that the PEG macroligands can be used for the formation of supramolecular star-shaped PEG. Further MALDI-TOF mass spectroscopy on the formation of grids based on **L5** or **L6** with metal ions could unfortunately not be obtained, presumably because of insufficient stability of the polymeric grids that are presumably fragmented at the high laser intensity. Interestingly, upon complexation of **L1** and **L5** there is an immediate appearance of the absorption band at 356 nm while for **L6** there is a more gradual change in the maximum absorption wavelength, indicating that the longer PEG chains suppress the cooperativity for grid formation, most likely due to the enhanced steric hindrance.

Conclusions

In conclusion, we have developed a versatile strategy for the synthesis of bis-tridentate metal coordinating ligands by CuAAc click reaction of 4,6-bis(6-ethynylpyridin-2-yl)-2-phenyl-pyrimidine with azido derivatives. The resulting 4,6-bis((1*H*-1,2,3-triazol-4-yl)-pyridin-2-yl)-2-phenylpyrimidine ligands **L1** and **L2** were demonstrated to self-assemble into metallosupramolecular grid-like complexes with Fe^{2+} and Zn^{2+} ions as was proven by ^{1}H-NMR and UV-Vis spectroscopy in combination with MALDI-TOF-MS. The macromolecular ligands were also successfully synthesized. The formation of the polymeric grids was found to be dependent on the structure of the polymer as [2x2] grid like supramolecular complexes could not be formed with the PEtOx macroligands **L3** and **L4**. However, self-assembly of the PEG macroligands (e.g., **L5**, and **L6**) with Fe^{2+} ions or Zn^{2+} ions resulted in the formation of star-shaped polymers by [2x2] grid-like metal complex formation. UV-Vis titration experiments have shown that in the initial stage complexes with two ligands and one Fe^{2+} are formed while at a later stage (i.e., after 0.25 eq of M^{2+}) a transition to grid-like complexes with four ligands and four Fe^{2+} ions is taking place. Furthermore, the large PEG-chains lower the cooperativity for grid-formation, ascribed to enhance steric hindrance. The reported synthetic route can be applied to a wide variety of azido end-functionalized polymers, leading not only to the development of new supramolecular star-shaped polymers but also forms the basis for new functional materials and hydrogels.

Conflicts of interest

There are no conflicts to declare.

Acknowledgements

X. Xu acknowledges the Chinese Scholarship Council (CSC, File No.201506780014) and Ghent University (BOF, File No. 01SC1717) for the financial support for his Ph.D program; R. Hoogenboom thanks FWO Flanders and Ghent Unviersity for continuous financial support. KVH thanks the Research Foundation – Flanders (FWO) (projects AUGE/11/029 and G099319N) for funding.

Notes and references

1. D. E. Barry, D. F. Caffrey and T. Gunnlaugsson, *Chem. Soc. Rev.*, 2016, **45**, 3244-3274.
2. A. J. McConnell, C. S. Wood, P. P. Neelakandan and J. R. Nitschke, *Chem. Rev.*, 2015, **115**, 7729-7793.
3. M. Ruben, J. Rojo, F. J. Romero-Salguero, L. H. Uppadine and J. M. Lehn, *Angew. Chem. Int. Ed. Engl.*, 2004, **43**, 3644-3662.
4. J.-F. Létard, P. Guionneau and L. Goux-Capes, *Spin Crossover in Transition Metal Compounds III*, 2004, 221-249.

5. B. Schneider, S. Demeshko, S. Dechert and F. Meyer, *Angew. Chem. Int. Ed.*, 2010, **49**, 9274-9277.
6. A. R. Stefankiewicz, G. Rogez, J. Harrowfield, M. Drillon and J.-M. Lehn, *Dalton Transactions*, 2009, 5787-5802.
7. M. T. Youinou, N. Rahmouni, J. Fischer and J. A. Osborn, *Angew. Chem.*, 1992, **104**, 771-773.
8. A. R. Stefankiewicz, G. Rogez, J. Harrowfield, M. Drillon and J. M. Lehn, *Dalton Trans*, 2009, DOI: 10.1039/b902262g, 5787-5802.
9. A. M. Madalan, X. Y. Cao, G. Rogez and J. M. Lehn, *Inorg. Chem.*, 2014, **53**, 4275-4277.
10. B. Schneider, S. Demeshko, S. Neudeck, S. Dechert and F. Meyer, *Inorg. Chem.*, 2013, **52**, 13230-13237.
11. D. E. Barry, C. S. Hawes, J. P. Byrne, B. la Cour Poulsen, M. Ruether, J. E. O'Brien and T. Gunnlaugsson, *Dalton Transactions*, 2017, **46**, 6464-6472.
12. M. S. Alam, S. Stromsdorfer, V. Dremov, P. Muller, J. Kortus, M. Ruben and J. M. Lehn, *Angew. Chem. Int. Ed. Engl.*, 2005, **44**, 7896-7900.
13. E. Breuning, M. Ruben, J. M. Lehn, F. Renz, Y. Garcia, V. Ksenofontov, P. Gütlich, E. Wegelius and K. Rissanen, *Angew. Chem.*, 2000, **112**, 2563-2566.
14. A. Semenov, J. P. Spatz, M. Möller, J.-M. Lehn, B. Sell, D. Schubert, C. H. Weidl and U. S. Schubert, *Angew. Chem. Int. Ed.*, 1999, **38**, 2547-2550.
15. D. M. Bassani, J. M. Lehn, S. Serroni, F. Puntoriero and S. Campagna, *Chemistry–A European Journal*, 2003, **9**, 5936-5946.
16. R. Hoogenboom, B. C. Moore and U. S. Schubert, *Macromol. Rapid Commun.*, 2010, **31**, 840-845.
17. N. G. White, J. A. Kitchen, J. A. Joule and S. Brooker, *Chem Commun (Camb)*, 2012, **48**, 6229-6231.
18. L. H. Uppadine, J. P. Gisselbrecht and J. M. Lehn, *Chem Commun (Camb)*, 2004, **6**, 718-719.
19. F. Robert, B. Tinant, R. Clérac, P.-L. Jacquemin and Y. Garcia, *Polyhedron*, 2010, **29**, 2739-2746.
20. M. Juríček, M. Felici, P. Contreras-Carballada, J. Lauko, S. R. Bou, P. H. J. Kouwer, A. M. Brouwer and A. E. Rowan, *J. Mater. Chem.*, 2011, **21**, 2104-2111.
21. M. H. Klingele and S. Brooker, *Coord. Chem. Rev.*, 2003, **241**, 119-132.
22. P. Thongkam, S. Jindabot, S. Prabpai, P. Kongsaeree, T. Wititsuwannakul, P. Surawatanawong and P. Sangtrirutnugul, *RSC. Adv.*, 2015, **5**, 55847-55855.
23. A. Mero, G. Pasut, L. D. Via, M. W. M. Fijten, U. S. Schubert, R. Hoogenboom and F. M. Veronese, *J. Controlled Release*, 2008, **125**, 87-95.
24. A. Joosten, Y. Trolez, J. P. Collin, V. Heitz and J. P. Sauvage, *J. Am. Chem. Soc.*, 2012, **134**, 1802-1809.
25. B. N. Gacal, V. Filiz and V. Abetz, *Macromol. Chem. Phys.*, 2016, **217**, 672-682.
26. G. Volet, T.-X. Lav, J. Babinot and C. Amiel, *Macromol. Chem. Phys.*, 2011, **212**, 118-124.
27. X. Xu, J. F. R. Van Guyse, V. V. Jerca and R. Hoogenboom, *Macromol. Rapid Commun.*, 2020, **41**, 1900305.
28. X. Xu, V. V. Jerca and R. Hoogenboom, *Macromol. Rapid Commun.*, 2020, **41**, 1900457.
29. R. Hoogenboom, D. Wouters and U. S. Schubert, *Macromolecules*, 2003, **36**, 4743-4749.
30. V. Aubert, V. Guerchais, E. Ishow, K. Hoang‐Thi, I. Ledoux, K. Nakatani and H. Le Bozec, *Angew. Chem. Int. Ed.*, 2008, **47**, 577-580.
31. X. Xu, F. A. Jerca, V. V. Jerca and R. Hoogenboom, *Adv. Funct. Mater.*, 2019, **29**, 1904886.

Graphic abstract

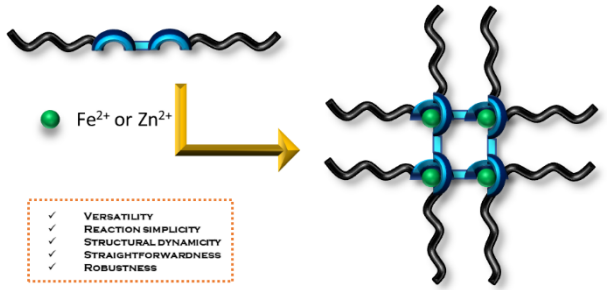

TOC text: [2 x 2] metallo-supramolecular grids were straightforwardly obtained by complexation of novel and well-designed 4,6-bis(6-ethynylpyridin-2-yl)-2-phenylpyrimidine analogue with Fe^{2+} or Zn^{2+} in organic medium, which outperforms the existing method in terms of robustness, versatility, reaction simplicity and straightforwardness, allowing for the synthesis of dynamic materials with diverse functionalities.